Peptides 31 (2010) 533–540

Contents lists available at ScienceDirect

Peptides

journal homepage: www.elsevier.com/locate/peptides

Synthesis, biophysical, and biological studies of wild-type and mutant psalmopeotoxins—Anti-malarial cysteine knot peptides from *Psalmopoeus cambridgei*

Pacharin Kamolkijkarn [1], Thitawan Prasertdee [1], Chawita Netirojjanakul, Pakornwit Sarnpitak, Somsak Ruchirawat, Songpon Deechongkit *

Laboratory of Medicinal Chemistry, Chulabhorn Research Institute, Chemical Biology Program, Chulabhorn Graduate Institute, Bangkok 10210, Thailand

ARTICLE INFO

Article history:
Received 2 November 2009
Received in revised form 3 January 2010
Accepted 3 January 2010
Available online 11 January 2010

Keywords:
Anti-malarial peptides
Biological information
Spectroscopic information
Disulfide peptide synthesis
Structure–activity relationship

ABSTRACT

Psalmopeotoxin I and II (PcFK1 and PcFK2), an anti-malarial peptide first extracted from *Psalmopoeus cambridgei* was synthesized and characterized. Both peptides belong to the Inhibitor Cystine Knot (ICK) superfamily, containing three disulfide bridges. The six cysteine residues are conserved similar to other members of the ICK superfamily, suggesting their critical role for either folding or function. In this study, the peptides were synthesized using Fmoc solid-phase peptide synthesis (SPPS). The three disulfide bonds of were constructed by regioselective and random oxidative approaches. The resulting disulfide bond patterns were verified by the HPLC-MS analysis of intact peptides and by the disulfide bond mapping using tryptic digestion. Implications of the disulfide bonds on the biophysical and biological properties of PcFKs were studied using three disulfide mutants in which a particular pair of cysteines was replaced with two isosteric serine residues. Structures and biophysical characteristics of all variants were studied using far-UV CD and fluorescence spectroscopy. Biological activities of all variants were evaluated using antiplasmodial assay against the K1 multi-drug-resistant strain of *P. falciparum*. The experimental results showed that the three disulfide bridges could not be correctly synthesized by the random oxidative strategy. Structural and biophysical analyses revealed that all variants had similar structures to the twisted β-sheet. However, the studies of disulfide bond removal indicated that each disulfide bond had different effects on both biophysical and biological activities of PcFKs. Correlation of biophysical parameters and biological activities showed that both PcFKs may have different mechanisms of actions for antiplasmodial activity.

1. Introduction

Malaria is one of the most common infectious diseases caused by parasites of the genus *Plasmodium*. There are over 200 species in this genus. *P. falciparum* is the most lethal form of the four malaria parasites and can be found globally. The infection mechanisms and pathology of malaria have been extensively studied and reviewed [16,19]. Due to malaria's prevalence, virulence, recrudescence, and resistance, there has been significant worldwide effort in finding new therapeutic agents for this disease. Recently, Camadro et al. identified two peptides, Psalmopeotoxin I and II (PcFK1 and PcFK2, Fig. 1), extracted from the venom of the Trinidad chevron tarantula, *Psalmopoeus cambridgei*. PcFK1 is a 33-residue peptide and PcFK2 is a 28-residue peptide (Fig. 1) [4]. Both have three disulfide bridges and belong to the Inhibitor Cystine Knot (ICK) superfamily [20]. The solution NMR structure of PcFK1 showed that the peptide has similar fold as other ICK family peptides with β-sheet and β-turn as major secondary structures (Fig. 1) [21]. Both peptides showed *in vitro* antiplasmodial activity (IC_{50} = 1–11 μM) against the intra-erythrocyte stage of *Plasmodium falciparum*. In addition, both peptides do not lyse erythrocytes or nucleate mammalian cells, and do not inhibit neuromuscular function [4]. These unique biochemical features of PcFKs make them the promising tools for malaria research. The aim of this study is to synthesize and characterize wild-type and disulfide mutants of PcFK1 and PcFK2. Structural analysis, biophysical characterization, and bioactivity assessment were conducted to correlate stability and efficacy data. These multi-disciplinary analyses provided insight into the rational design of peptides aiming to optimize biological functions.

* Corresponding author. Tel.: +66 86122 6641.
E-mail address: songpond@gmail.com (S. Deechongkit).
[1] These authors contributed equally to this work.

0196-9781/$ – see front matter © 2010 Elsevier Inc. All rights reserved.
doi:10.1016/j.peptides.2010.01.001

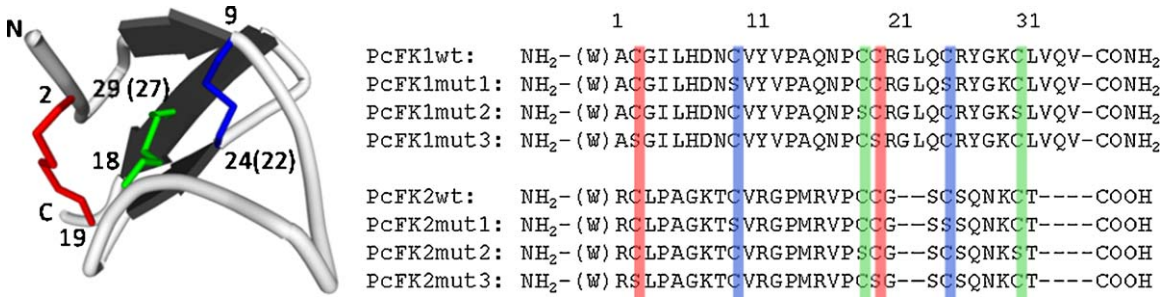

Fig. 1. Solution NMR structure (PDB ID: 1H5V) and sequences of PcFK wild-type and disulfide mutants.

2. Materials and methods

2.1. Materials

All Fmoc-protected amino acids, solid support, and peptide synthesis chemical reagents were purchased from Novabiochem (San Diego, CA, U.S.A.), Sigma–Aldrich–Fluka (St Louis, MO, U.S.A.), and Peptide Institute Inc. (Osaka, Japan). Buffer solutions used for biophysical studies were 10 mM of glycine–HCl (pH 3), sodium acetate (pH 4), sodium phosphate (pH 6, 7.4, 11, 12), and TRIS–HCl (pH 9).

2.2. General method for solid-phase peptide synthesis (SPPS)

Construction of linear PcFK wild-type and disulfide mutants were carried out by manual Fmoc solid-phase peptide synthesis. Rink amide and Wang resin were used for PcFK1 and PcFK2, respectively. All syntheses were performed on a 0.1–0.4 mmole scale, the coupling reaction was carried out using 4 equiv. of amino acid and the activating agent 2-(1*H*-benzotriazol-1-yl)-1,1,3,3-tetramethyluronium hexafluorophosphate (HBTU, 4 equiv.) and 1-hydroxybenzotriazole (HOBt, 4 equiv.) in the presence of diisopropylethylamine (DIEA, 8 equiv.) for 30 min. The N-terminal Fmoc deprotection was achieved using 20% piperidine in DMF for 30 min. Cleavage from resin and side-chain deprotection were achieved using 1 mL of reagent K per 0.025 mmole of crude peptide (reagent K: 82.5% TFA, 5% thioanisole, 5% *m*-cresol, 5% water, and 2.5% ethanedithiol) for 4 h at room temperature. The resulting crude peptides were purified by preparative reversed-phase HPLC. Purity of all peptides was confirmed by analytical RP-HPLC and identity of all peptides was confirmed by ESI-HRMS (Bruker Daltonics, Bellerica, MA, U.S.A.) shown in Table 1.

2.3. Purification and identification

RP-HPLC was performed on Young Lin Instrument Acme 9000 system (Seoul, Korea) equipped with binary pump and UV detector. Stationary phase was Vydac C18 column. The mobile phase system was water–acetonitrile (ACN)–trifluoroacetic acid (TFA). Flow rates were 1 and 10 mL/min for analytical and preparative HPLC, respectively. Chromatograms were monitored at 230 and 280 nm, unless indicated otherwise.

2.4. Regioselective disulfide bond formation

Each disulfide bond was formed after cleavage and deprotection of the relevant linear peptides with Cys' protecting groups shown in Table 1 following three major steps described below.

2.4.1. The first intramolecular disulfide bond formation (Monodisulfide, MDS)

Since the two Trt side-chains protecting groups of cysteine (Cys) were removed at the same time as peptide cleavage from the resin. The first disulfide bond can be formed using 0.95 equiv. of 2,2′-dithiodipyridine (PySSPy) and 1 mM peptide in 0.1% (v/v) TFA in water at room temperature. The oxidation was completed after 2 h and product was purified by preparative RP-HPLC. The product was identified by ESI-MS. The typical yield for this reaction was 60–75%.

2.4.2. The second intramolecular disulfide bond formation (Didisulfide, DDS)

The 1 mM peptide-MDS in 99% TFA and 1% anisole (v/v) was treated with 200 equiv. of silver trifluoroacetate (AgOTfa) and 200 equiv. of trifluorometanesulfonic acid (TfOH) which formed silver triflate in situ, stirred for 2 h at room temperature. Peptide silver salt was precipitated in ice-cold *tert*-butyl methyl ether (MTBE, 0 °C), centrifuged at 20,000 rpm for 10 min, re-dissolved in 30% ACN 0.1% TFA, and treated with 0.67 equiv. of PySSPy for 8–16 h at room temperature. The resulting crude product was purified by preparative RP-HPLC. The product was identified by ESI-HRMS (Table 1). The typical yield for this reason was 65–70%.

2.4.3. The third intramolecular disulfide bond formation (Tridisulfide, TDS)

The peptide-DDS in TFA was treated with TfOH and thioanisole (10:1:1, v/v/v), stir at 0 °C for 1 h. After the reaction was completed, the reaction mixture was immediately purified in single injection by preparative RP-HPLC as described above. The product was identified by ESI-MS. The third disulfide bond can be formed using 0.95 equiv. of PySSPy in 1 mM peptide 0.1% (v/v) TFA in water for 8–16 h at room temperature. The resulting crude product was purified by preparative RP-HPLC. The final product was identified by ESI-HRMS (Table 1). The typical yield for both steps was 35–45%. It was also found that using anisole in place of thioanisole could afford the same products with similar yields, but could lead to an easier purification.

2.5. Random oxidative disulfide bond formation

The PcFK(wt) containing six free thiol groups (1 mM) were reacted with 2.85 (3×0.95) equiv. of PySSPy in 0.1% (v/v) TFA in water for 8–16 h at room temperature. The resulting crude products were purified by preparative RP-HPLC. The final products were identified by ESI-MS. Typical yield for multiple disulfide bond formation step only was 30–40%. A different approach using glutathione was described elsewhere [3].

2.6. Comparative analytical HPLC study

Analytical HPLC was conducted as described above. The gradient used was 0–40% B (solution B, 100% ACN 0.1% TFA) for 45 min with 2 min pre-gradient. For each type of PcFK; PcFK prepared by regioselective disulfide bond formation (PcFK), PcFK prepared by random oxidation (PcFK′), and the mixture of both types of PcFK (PcFK + PcFK′) were run separately and fraction

Table 1
Summary of PcFK variants, MS data, and bioactivity data.

	Mutations/modifications	Cysteine protecting groups			Expected mass (Da)	Observed mass (Da)	IC_{50}		% [^{3}H] Uptake at different [protein]			
		Trt	Acm	*t*Bu			μg/mL	μM	20 μg/mL	10 μg/mL	2 ng/mL	1 μg/mL
PcFK1	Regioselective S-S formation	C9, C24	C18, C29	C2, C19	3802.7457	3802.7232	n.d.	n.d.	59.4	86.4	93.0	84.4
PCFK1[1]	Random oxidative S-S formation	C2, C9, C18, C19, C24, C29	–		3802.7457	3802.6567	n.d.	n.d.	97.2	95.3		
PcFK1 mud	C9S and C24S	C18, C29	C2, C19	–	3772.8071	3772.6805	n.d.	n.d.	62.7	83.6		
PcFK1 mut2	C18S and C29S	C9, C24	C2, C19		3772.8071	3772.5712	n.d.	n.d.	87.3	91.8	84.8	88.8
PcFK1 mut3	C2S and C19S	C9, C24	C18, C29	–	3772.8071	3772.4613	n.d.	n.d.	65.4	71.4		
PcFK2	Regioselective S-S formation	C9, C22	C18, C27	C2, C19	3135.3797	3135.3772	9.2 ± 2.5	2.7 ± 0.8	37.8	48.2	90.8	86.8
PCFK2[1]	Random oxidative S-S formation	C2, C9, C18, C19, C22, C27	–		3135.3797	3135.3212	n.d.	n.d.	101.0	96.2		
PcFK2 mud	C9S and C22S	C18, C27	C2, C19	–	3105.4411	3105.1693	n.d.	n.d.	72.7	82.2	91.0	85.3
PcFK2 mut2	C18S and C27S	C9, C22	C2, C19		3105.4411	3105.2620	n.d.	n.d.	67.9	74.8	89.8	86.8
PcFK2 mut3	C2S and C19S	C9, C22	C18, C27	–	3105.4411	3105.2698	n.d.	n.d.	87.8	85.4	91.3	86.5

collected to confirm mass of the eluted peptides. The chromatograms and MS characteristics were compared.

2.7. Circular dichroism study

Circular dichroism (CD) experiments were performed on Jasco J-815 CD Spectropolarimeter (Tokyo, Japan) with peltier temperature-controlled cell holder using a 0.2 cm cuvette. For the far-UV CD wavelength scan, the spectra were recorded from 260 to 190 nm at 25 °C. CD spectra were collected using a step-resolution of 0.1 nm, scanning speed of 20 nm/min, and 1-nm bandwidth. Samples were 8.0–10.0 μM peptide in 10 mM buffers (pH 3–12). All the CD spectra were baseline corrected by subtraction with the buffer recorded under the same conditions and were normalized to 10 μM.

2.8. Flurorescence study

Fluorescence experiments were performed on PTI fluorescence spectrophotometer (Birmingham, NJ, U.S.A.). Intrinsic fluorescence emission spectra were obtained using an excitation wavelength at 280 nm. All fluorescence spectra were recorded from 300 to 400 nm at 25 °C. The temperature was controlled using a Quantum Northwest TC 125 peltier temperature controller. Peptide concentrations ranged from 2.0 to 3.0 μM in 10 mM buffer (pH 3–12). All fluorescence spectra were normalized into 2 μM.

2.9. Thermal unfolding study

The far-UV CD, wavelength/temperature scan macro was employed. Samples were 8.0–10.0 μM peptide in 10 mM buffer (pH 3–12). Temperature scans of the samples were achieved by heating the samples from 0 to 100 °C using 2 °C/min heating rate. The change in protein characteristics was monitored at 214 nm with 8 s response time. In addition, wavelength scans for the samples were taken every 5 °C using the same parameter as the wavelength scan mentioned above. After the highest temperature was reached, samples were cooled to 25 °C and then another wavelength scan was collected to determine degree of reversibility. Fraction unfolding (f_u) curve was determined using the baseline extrapolation method. The mid-point of temperature transition (T_m) was calculated from the fraction unfolding curve.

2.10. Biological activity study

PcFK, PcFK′ (wild-type), and PcFK disulfide mutants were subjected to the measurement of *in vitro* activity testing of potential anti-malarial drugs, against the intra-erythrocyte stage of *P. falciparum*. *P. falciparum* (K1, multi-drug resistant strain) was used by culturing in RPMI 1640 medium containing 20 mM HEPES (*N*-2-hydroxyethylpiperazine-*N*′-2-ethanesulfonic acid), 32 mM $NaHCO_3$, and 10% heat activated human serum with 3% erythrocytes. The culture was incubated at 37 °C in an incubator with 3% CO_2. Increasing concentrations of the peptides in the medium (1 μg/mL, 2 μg/mL, 10 μg/mL and 20 μg/mL) were distributed in a 96-microwell plate for assaying the dose–response. Quantitative assessment of anti-malarial activity was determined by microculture radioisotope techniques based upon the methods described by Desjardins et al. [9]. Levels of incorporated radioactively labeled [^{3}H]hypoxanthine indicating parasite growth was determined using the TopCount microplate scintillation counter (Packard, Fullerton, CA, U.S.A.). Inhibition concentration (IC_{50}) represents the concentration where 50% reduction in parasite growth is observed. The standard sample is Dihydroartemisinine (DHA).

3. Results

3.1. Sequence design and experimental rationale

The sequences for PcFK wild-type and disulfide mutants were shown in Fig. 1. An additional Trp (W) was added to the N-terminus as a means to measure protein concentration, both for molarity needed during synthesis and for subsequent biophysical and biological studies. For the mutants, each disulfide bond of PcFKs was removed by Cys-to-Ser substitutions. The peptide identities were confirmed by ESI-HRMS (Table 1). Secondary and tertiary structures were assessed by far-UV circular dichroism (CD) and intrinsic fluorescence, respectively. Stability was assessed by CD thermal unfolding using a baseline extrapolation method [12]. Lastly, bioactivity was assessed using antiplasmodial assay described by Desjardin et al., which monitored growth of *P. falciparum* (K1, multi-drug resistant strain) during intra-erythrocyte stage by [G-^{3}H] hypoxanthine uptake [9].

3.2. Regioselective and random oxidative approaches to synthesize PcFKs

The syntheses of ICK peptides are usually complicated due to the presence of multiple disulfide bonds in the same linear peptide chain [1,5]. Previous syntheses employed vastly different approaches for disulfide bond formation after solid-phase peptide synthesis of the linear peptides [6,11,23]. However, the multiple disulfide bond formation processes can be divided into two distinct strategies. First, regioselective strategy employs orthogonal protecting groups to form each disulfide bond one at a time [1,2,5]. Second, random oxidative strategy allows all the disulfide bonds to form simultaneously in the presence of 2,2′-dithiodipyridine (PySSPy). Scheme 1A and B shows the synthesis of PcFKs by regioselective and random oxidative strategies, respectively. The selections of Cys protecting groups for each strategy were shown in Table 1. The peptides synthesized by regioselective strategy were called PcFK1 and PcFK2, while the peptides synthesized by random oxidative strategy were called PcFK1′ and PcFK2′. The resulting peptides were compared based on reverse phase HPLC (RP-HPLC) profiles, secondary structure by far-UV CD, tertiary structure by intrinsic fluorescence as shown in Fig. 2, and antiplasmodial activities shown in Table 1. PcFKs from both strategies had different polarity based on differences in retention times of RP-HPLC. Moreover, the PcFK1 and PcFK1′ may interact with one another to further undergo disulfide bond scrambling leading to a new co-eluting peak when co-injecting both PcFK1 and PcFK1′ (Fig. 2A, dotted line). CD and fluorescence showed different spectroscopic properties. Most importantly, PcFKs from regioselective strategy were more bioactive and had bioactivity similar to those of natural PcFKs, while those from random oxidative strategy were not. Moreover, tryptic peptide mapping indicated that regioselective strategy gave the expected fragments of the correct disulfide patterns (see ESI-HRMS, observed mass [M+H] for major fragment of PcFK1: 3494.4572 Da and for major fragment of PcFK2: 2406.9703 Da), while random oxidative strategy did not. Furthermore, each disulfide bond was formed sequentially after the confirmation that all the cysteines became cystines by LC-MS. All the reaction conditions and storage solutions for the intermediates were under highly acidic condition, thus disulfide bond scrambling was not possible. These results indicated that each disulfide bond of PcFKs must be formed sequentially to ensure proper folding and function.

3.3. Biophysical studies

Far-UV CD at pH 3 (Fig. 2), the pH where NMR structure was derived, showed that PcFK(wt)'s adopted twisted β-sheet conformation with λ_{max} around 225 nm and λ_{min} around 200 nm [14]. Far-UV CD signal was not strong since ~50% of PcFK(wt)'s were unstructured. Thermal unfolding curves of the two peptides were broad, indicating that heat capacity upon unfolding was low as a result of small hydrophobic core in these peptides. The CD characteristics of PcFK(wt)'s at pH 7.4 showed similar trends as those at pH 3. However, the stability at pH 7.4 was lower than that at pH 3. The fluorescence emission data (Fig. 3C) mostly arose from Trp. PcFK1(wt) has Tyr, but PcFK2(wt) does not. Yet, Tyr emission was overwhelmed. Therefore, the fluorescence spectra mostly showed the local structure and nearby hydrophobic core, and thus did not influence the overall biophysical analysis. The thermal unfolding data for both wild-type and disulfide mutants were shown in Fig. 4. Generally, the removal of a disulfide bond destabilized PcFK's. The effects of each disulfide bond on stability were different.

3.4. Bioactivity studies

Antiplasmodial activity of PcFK(wt)'s (Table 1) varied slightly from the literature, but were in similar range (1–11 μM) [4,21].

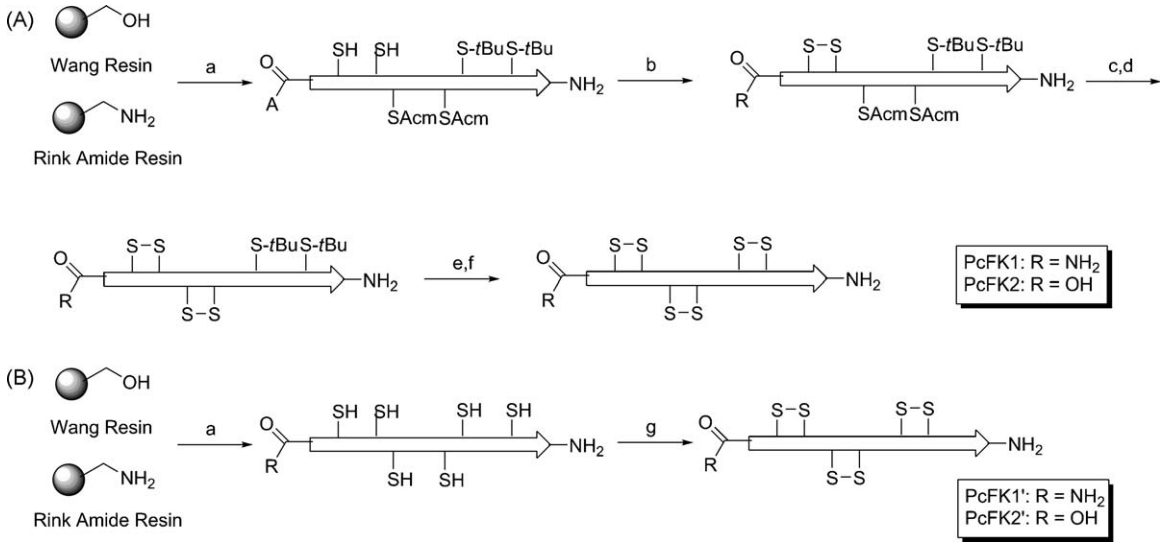

Scheme 1. (A) Synthesis of PcFK by regioselective disulfide formation and (B) synthesis of PcFK′ by random oxidative disulfide formation.

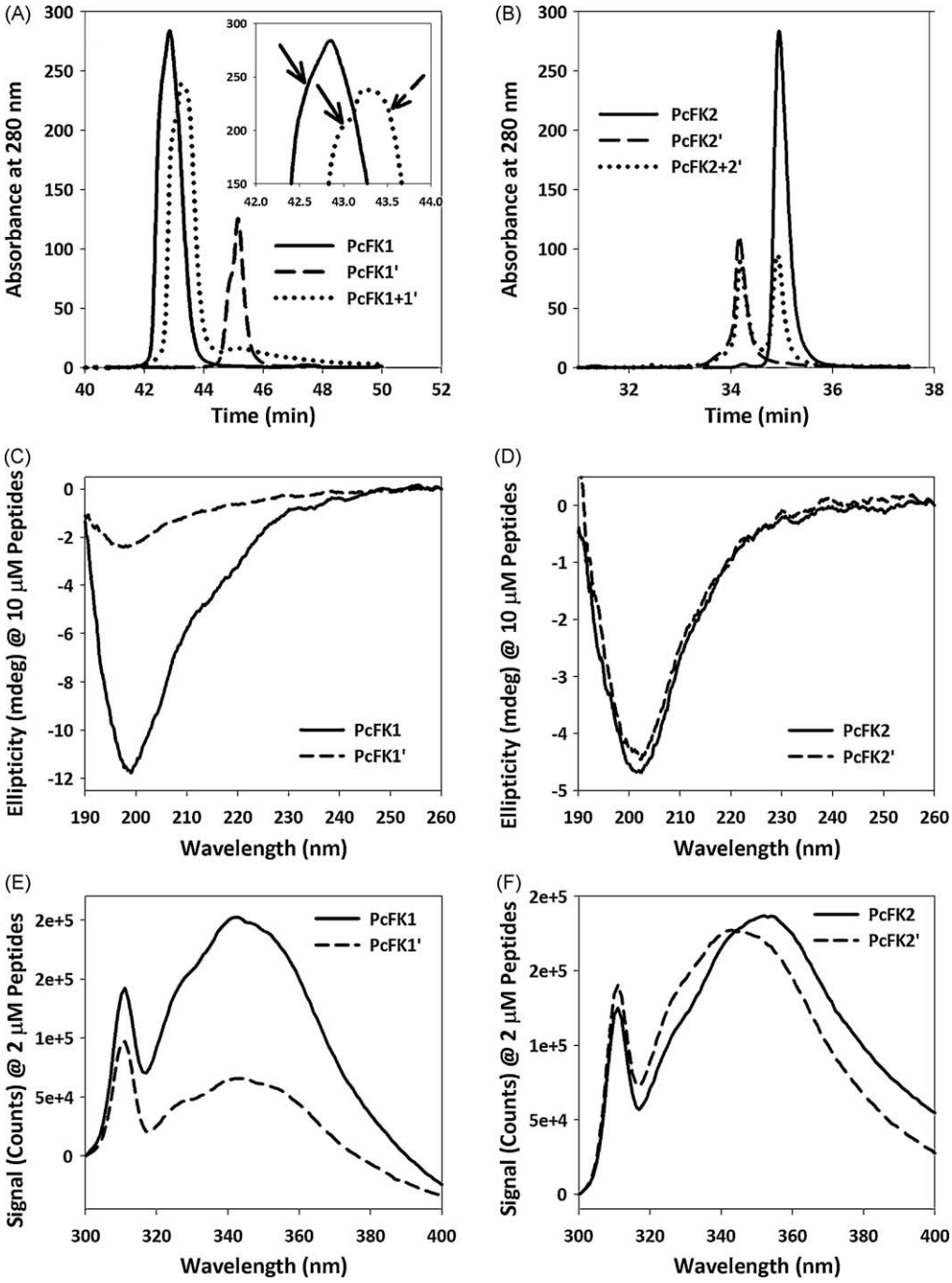

Fig. 2. Overlays of chromatograms of (A) PcFK1 and (B) PcFK2, each figure overlays injections of PcFK, PcFK′, and PcFK + PcFK′ co-injections. Overlay of CD spectra at pH 3 of PcFK and PcFK′ of (C) PcFK1 and (D) PcFK2. Overalay of fluorescence spectra at pH 3 of PcFK and PcFK′ of (E) PcFK1 and (F) PcFK2. The arrows in the inset of (A) indicated the presence of PcFK1 (solid arrow) and PcFK1′ (dashed arrow).

The variation could result from different *P. falciparum* strains. Generally, PcFK2(wt) had higher antiplasmodial activity than PcFK1(wt). The disulfide mutants had lower bioactivity than their respective wild-types, and the bioactivity for all variants were on the low end (>20 mg/mL).

4. Discussion

4.1. Comparing regioselective and random oxidative disulfide bond formation for synthesis of PcFKs

Though some peptides containing multiple disulfide bonds have been synthesized by random oxidative, the success depended on whether these peptides were already structured or had conformational propensity to adopt the native structure, with or without stability contributions from disulfide bonds. In the case of cyclotides, a related family of multiple disulfide bond peptides with cyclised backbone, these peptides were partially stabilized by backbone cyclization [8] prior to random oxidative disulfide bond formation in addition to their inherent propensity to form the cyclotide folds [3,25,26]. In some cases, oxidative refolding approach to form multiple disulfide bonds by using air oxidation in the presence of glutathione was employed. In this study, the air oxidation in the presence of glutathione was also tried. However, the reaction time was longer than the reaction with PySSPy, and the resulting PcFKs from reaction with glutathione or with PySSPy

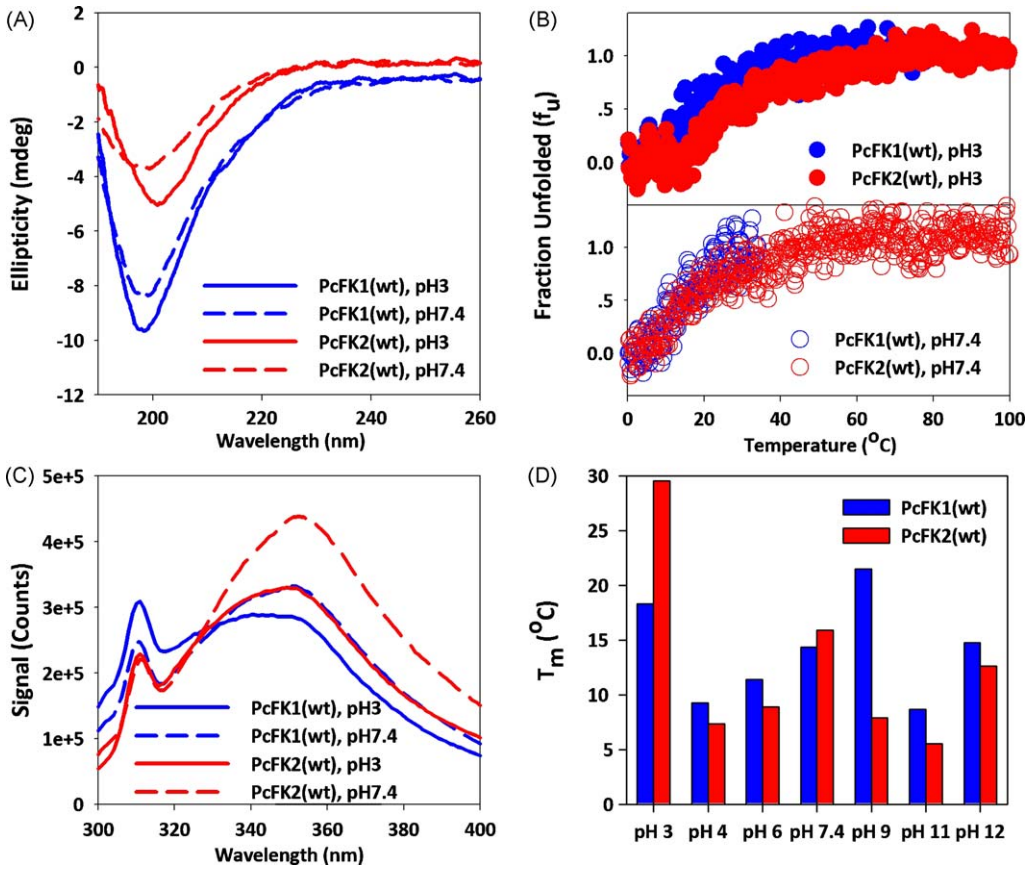

Fig. 3. (A) Overlay of CD spectra at 5 °C of PcFK1(wt) and PcFK2(wt) at pH 3 and pH 7.4. (B) Overlay of thermal unfolding curves monitored by CD of PcFK1 and PcFK2 at pH 3 (top) and pH 7.4 (bottom). (C) Overlay of fluorescence spectra at 6 °C of PcFK1(wt) and PcFK2(wt) at pH 3 and pH 7.4. (D) Summary of T_m monitored by CD for PcFKs(wt) at different pH.

both gave different peptides from regioselective approach as confirmed by RP-HPLC (data not shown). Under random oxidative condition, HPLC profile showed only one peak of full length peptide instead of an array of peptides with the same mass, as shown in Fig. 2A and B. Without any thermodynamic (conformational) preference at the condition for PySSPy reaction, the kinetic would afford the products in which each disulfide bond was formed between pairs of the nearest cysteines as confirmed by tryptic digestion analysis (i.e. PcFK1: C2-C9, C18-C19, C24-C29 resulting in observed mass of major fragments [M+H] at 1134.5700 and 2358.9504 Da; and PcFK2: C2-C9, C18-C19, C22-C27, resulting in observed mass of major fragments [M+H] at 460.2401, 1063.5645 and 1343.5176 Da, see supporting information for expected mass of major fragments). Camadro et al. also employed simultaneous disulfide bond formation approach to form all three disulfide bonds of PcFK1 derived from recombinant protein expression [4,7,21]. They found that the approach yielded both native PcFK1 and PcFK1 with incorrect disulfide bond patterns [7]. They also identified that the incorrect form of PcFK1 had similar disulfide pattern as the one observed by random oxidation in our study. These results supported our study that random oxidative strategy or similar approaches may not be universally successful for the synthesis of peptide containing multiple disulfide bonds. Though random oxidative approach is more convenient than regioselective approach, its utility is likely limited to peptides whose stability native folds are less dependent on the presence of disulfide bond. The failure of random oxidative strategy for PcFK synthesis could also imply that PcFKs were not as structured as other peptides—the implication which was further corroborated by biophysical results.

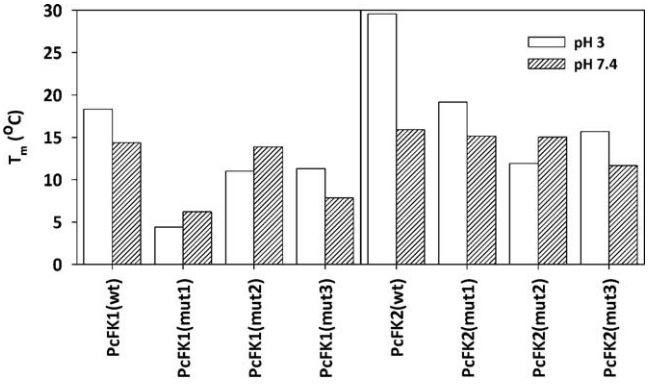

Fig. 4. Comparisons of T_m for all PcFKs variants at pH 3 and 7.4.

4.2. Biophysical analysis of wild-type and mutant PcFKs

The two peptides showed different CD thermal stability, in which PcFK2(wt) had mid-point of unfolding (T_m) at 29.6 °C compared to 18.3 °C of PcFK1(wt). Theoretical protein charge calculation showed that PcFK2(wt) (+6) was more charged than PcFK1(wt) (+4.5) at pH 3 [15]. Therefore, the stabilization from solvation effect for PcFK2 was more dominant than that for PcFK1, and the observed effect was the most evident at pH 3 [10,24]. Secondly, the loop linking the first two β-strands for PcFK2(wt) (residues 10–20) were shorter than that for PcFK1(wt) (residues 10–22), making hydrophobic cluster of PcFK2(wt) more compact.

The differences in T_m's between wild-types at other pH's were not as drastic as those at pH 3. Generally, stability of PcFK2(wt) drastically dropped after pH 3 due to lower charge and

consequently lower solvation effect, whereas PcFK1(wt) had similarly low stability over broader range of pH. This result indicated that the impact of the loop between β-strands 1 and 2 was more critical to stability than protein charge and solvation effect. In addition to pH 3, pH 7.4 seemed to have distinguishable value of T_m in the pH range of 4–12. These results could come from the charge neutralization at either terminus which could make termini less demanding to be solvent exposed, allowing the flexible region near either terminus to be more structured. Lastly, the anomalously high T_m's for PcFK1 at pH 9 (p*I* = 9.6) and PcFK2 at pH 12 (p*I* = 12.3) were likely the results of isoelectric precipitation (precipitates observed when heating samples at pH near p*I*).

The mutant data (Fig. 4) showed that removal of disulfide bond reduced the stability of PcFKs. For PcFK1, the disulfide bond between C9 and C24 was the most important. Its absence means that the peptide from G3 to P18 was attached to the core structure likely only by hydrophobic core. Since this region has long loop which reduced stability of PcFK1(wt) when compared to PcFK2(wt), the hydrophobic core in this region should be unstable. Therefore, without stabilization from C9-C24 disulfide bond, PcFK1(mut1) became largely unfolded. For PcFK2, the least stable mutants are mut2 at pH 3 and mut3 at pH 7.4. Because both mut2 and 3 involved peptide segment near either N- or C-termini, the peptide segment would be detached from the core structure upon removal of the respective disulfide bonds. Nonetheless, PcFK2 mutants had stability similar to that of PcFK1(wt). This result means that the hydrophobic core of PcFK2 was more optimized than PcFK1. When compared to PcFK1, the relatively more stable hydrophobic core of PcFK2 was also the likely explanation for the low impact of disulfide bond removal at pH 7.4, where stability from hydrophobic core dominated. These biophysical results suggested that PcFK2 may have evolved from PcFK1 in order to achieve greater thermal stability.

4.3. Bioactivity studies, structure–activity relationship, and possible mechanisms of action

Considering the thermal unfolding data, PcFK(wt)'s were largely populated by unfolded states at the condition of bioassay (37 °C at pH 7.4). While both folded and unfolded forms of PcFK(wt)'s could be bioactive, the fact that PcFK2(wt) was more bioactive suggested that only the folded state might be the more bioactive form. The analyses and applications of structure–activity relationship (SAR) of peptides have been studied extensively to gain insight into mechanism of action, target–peptide interaction, and design of optimized peptide ligands [13,17,18,22,27]. If the targets of the peptides and the structural information of both the targets and the peptides were available, then a more classical and extensive SAR analysis can be conducted. In this case, however, the target was not known and the structural information for PcFKs was limited. In this study, the biophysical parameters along with the available NMR solution structure of PcFK1 were used in place of the more refined structural information under the assumption that the structures of PcFK1 and PcFK2 were similar. This assumption was likely valid since cysteine knot peptides tend to have the same folding motif [20]. This study used T_m's as the representative parameter for PcFK structures. The rationale for using T_m data was two folds. First, the T_m data were

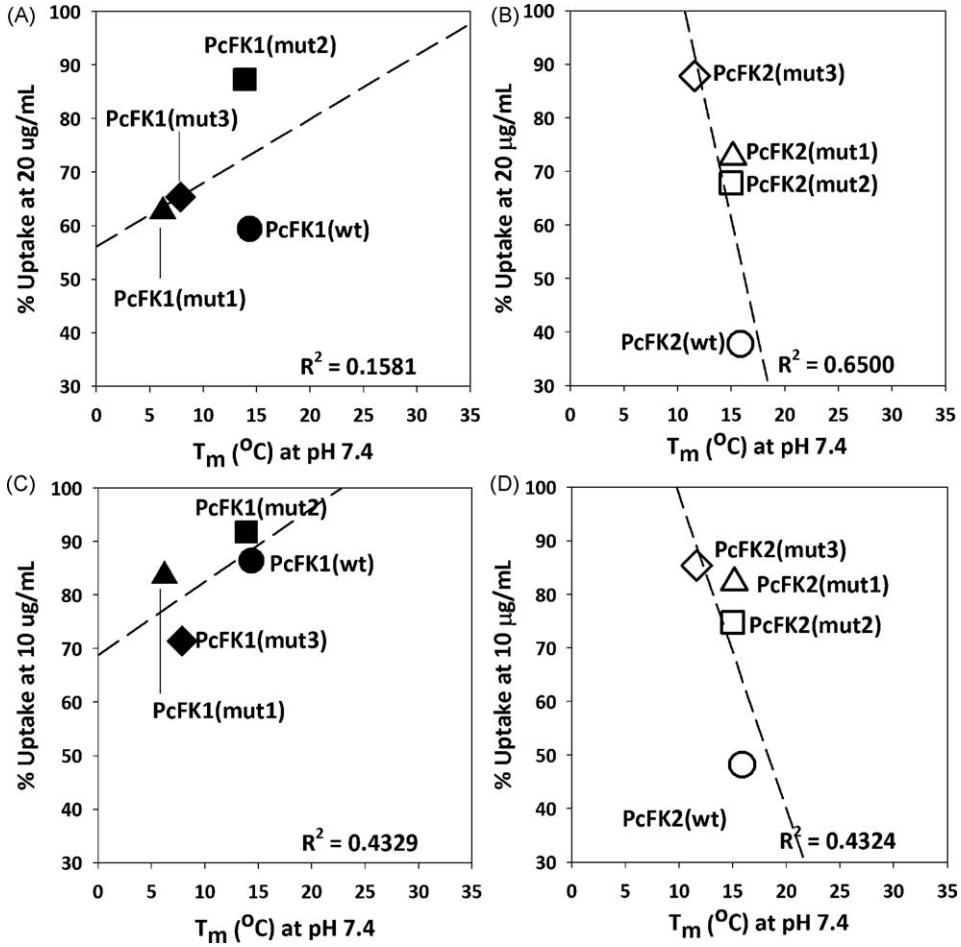

Fig. 5. Correlation between T_m's at pH 7.4 and % uptake at 20 μg/mL for PcFK1 variants (A) and PcFK2 variants (B); and Correlation between T_m's at pH 7.4 and % uptake at 10 μg/mL for PcFK1 variants (C) and PcFK2 variants (D).

derived based on relative population of folded and unfolded state at different temperature. Second, the difference in T_m's among variants can be explained based on the available structural model. In other words, T_m's implicitly described the structure of each PcFK variant as a result of mutation—in this case disulfide bond removal. Thus, the impact of disulfide bond on bioactivity could be assessed. For these reasons, bioactivity and thermal stability were employed to correlate under the framework of structure–activity relationship. Fig. 5 shows the correlation of T_m at pH 7.4 and % uptake at 10 and 20 μg/mL peptides for all variants. Ideally, the T_m should be correlated with IC_{50}. Because IC_{50} data for most of the variants were high, the % uptake at 10 and 20 mg/mL were used instead. Generally, the trends of T_m vs. % uptake were similar at either peptide concentration, further ensuring the reliability of the observed trends.

There are two observations when compared the SAR between PcFK1 and PcFK2. First, the bioactivity of PcFK1 variants was not sensitive to T_m except for PcFK1(mut2), while the bioactivity of PcFK2 variants was particularly sensitive to T_m at pH 7.4. Second, the disulfide mutants of PcFK1 were more bioactive than those of PcFK2, except for PcFK1(mut2). These observations suggested that PcFK1 and PcFK2 may have different modes of action or targets in *P. falciparum*. For PcFK1, the peptide may already contain important resides for binding, thus the lack of conformational stability did not obliterate the bioactivity. Those residues of PcFK1 could be in the region near the disulfide bond between C18-C29 as indicated by the anomalously low activity of PcFK1(mut2). In contrast, the conformation of PcFK2, either in addition to or instead of, the specific residues, was critical for binding, thus reducing the folded state population greatly impacted the bioactivity.

5. Conclusion

PcFKs can be synthesized by solid-phase peptide synthesis. Due to its low conformational stability, the regioselective, rather than random oxidative, disulfide strategy, was preferred. PcFK2 generally had more favorable biophysical characteristics and antiplasmodial activity than PcFK1, making PcFK2 a better candidate for stability and bioactivity optimization. Finally, the analysis of structure–activity relationship using biophysical parameters as substitutes for actual structural information provided insight into possible mode of actions for both PcFKs. In absence of detailed structural information for peptides or proteins, relatively difficult information to obtain for biomacromolecules, biophysical characterization may substitute for the structural information, typically used for small molecule development. For the future, more mutations will be studied to further probe the mechanism of action and subsequently the target(s) of PcFKs. Such studies include the classical alanine scan or truncation to probe the pharmacophores. Since PcFKs may also have ion channel modulation properties, PcFKs in combination with existing anti-malarial drugs will be assessed whether it may enhance activity of those drugs.

Acknowledgements

We thank Chulabhorn Foundation, Thailand Research Fund (RSA5180007), and ETM (Center on Environmental Health, Toxicology and Management of Toxic Chemicals) for funding, N. Chimnoi for mass spectrometry assistance, and S. Veeranondha, W. Choowong, K. Intereya of Bioassay Laboratory of National Biotechnology Center of Thailand (BIOTEC) for conducting antiplasmodial assay, Professor Philip E. Dawson and Professor Evan T Powers of The Scripps Research Institute (La Jolla, CA) for helpful advice, and Professor Jeffery W. Kelly Laboratory at The Scripps Research Institute (La Jolla, CA) and Protein Formulation Group at Amgen Inc. (Thousand Oaks, CA) for generous gifts of special laboratory supplies for peptide synthesis, purification, and characterization.

Appendix A. Supplementary data

Supplementary data associated with this article can be found, in the online version, at doi:10.1016/j.peptides.2010.01.001.

References

[1] Akaji K, Fujino K, Tatsumi T, Kiso Y. Total synthesis of human insulin by regioselective disulfide formation using the silyl chloride-sulfoxide method. J Am Chem Soc 1993;115:11384–92.
[2] Bathgate RA, Lin F, Hanson NF, Otvos Jr L, Guidolin A, Giannakis C, et al. Relaxin-3: improved synthesis strategy and demonstration of its high-affinity interaction with the relaxin receptor LGR7 both in vitro and in vivo. Biochemistry 2006;45:1043–53.
[3] Cemazar M, Daly NL, Haggblad S, Lo KP, Yulyaningsih E, Craik DJ. Knots in rings. The circular knotted protein Momordica cochinchinensis trypsin inhibitor-II folds via a stable two-disulfide intermediate. J Biol Chem 2006;281:8224–32.
[4] Choi SJ, Parent R, Guillaume C, Deregnaucourt C, Delarbre C, Ojcius DM, et al. Isolation and characterization of Psalmopeotoxin I and II: two novel antimalarial peptides from the venom of the tarantula Psalmopoeus cambridgei. FEBS Lett 2004;572:109–17.
[5] Cline DJ, Thorpe C, Schneider JP. General method for facile intramolecular disulfide formation in synthetic peptides. Anal Biochem 2004;335:168–70.
[6] Coin I, Beyermann M, Bienert M. Solid-phase peptide synthesis: from standard procedures to the synthesis of difficult sequences. Nat Protoc 2007;2:3247–56.
[7] Combes A, Choi SJ, Pimentel C, Darbon H, Waidelich D, Mestivier D, et al. Determination with matrix-assisted laser desorption/ionization tandem time-of-flight mass spectrometry of the extensive disulfide bonding in tarantula venom peptide psalmopeotoxin I. Eur J Mass Spectrom 2009;15:517–29.
[8] Daly NL, Clark RJ, Craik DJ. Disulfide folding pathways of cystine knot proteins. Tying the knot within the circular backbone of the cyclotides. J Biol Chem 2003;278:6314–22.
[9] Desjardins RE, Canfield CJ, Haynes JD, Chulay JD. Quantitative assessment of antimalarial activity in vitro by a semiautomated microdilution technique. Antimicrob Agents Chemother 1979;16:710–8.
[10] Dill KA. The meaning of hydrophobicity. Science 1990;250:297–8.
[11] Fields GB, Noble RL. Solid phase peptide synthesis utilizing 9-fluorenylmethoxycarbonyl amino acids. Int J Pept Protein Res 1990;35:161–214.
[12] Gursky O, Atkinson D. Thermodynamic analysis of human plasma apolipoprotein C-1: high-temperature unfolding and low-temperature oligomer dissociation. Biochemistry 1998;37:1283–91.
[13] Horwell DC. Use of the chemical structure of peptides as the starting point to design nonpeptide agonists and antagonists at peptide receptors: examples with cholecystokinin and tachykinins. Bioorg Med Chem 1996;4:1573–6.
[14] Jager M, Nguyen H, Crane JC, Kelly JW, Gruebele M. The folding mechanism of a beta-sheet: the WW domain. J Mol Biol 2001;311:373–93.
[15] Laue TM, Shah BD, Ridgeway TM, Pelletier SL. Computer-aided interpretation of analytical sedimentation data for proteins. In: Harding SE, Rowe AJ, Horton JC, editors. Analytical ultracentrifugation in biochemistry and polymer science. Cambridge, United Kingdom: The Royal Society of Chemistry; 1992. p. 90–125.
[16] Mendis K, Sina BJ, Marchesini P, Carter R. The neglected burden of Plasmodium vivax malaria. Am J Trop Med Hyg 2001;64:97–106.
[17] Nielsen KJ, Schroeder T, Lewis R. Structure–activity relationships of w-conotoxins at N-type voltage-sensitive calcium channels. J Mol Recognit 2000;13:55–70.
[18] Nishio H, Katoh E, Yamazaki T, Inui T, Nishiuchi Y, Kimura T. Structure–activity relationships of calcicludine and dendrotoxin-I, homologous peptides acting on different targets, calcium and potassium channels. Biochem Biophys Res Commun 1999;262:319–21.
[19] Olliaro PL, Bloland PB. Clinical and public health implications of antimalarial drug resistance. Antimalarial Chemother 2001;65–83.
[20] Pallaghy PK, Nielsen KJ, Craik DJ, Norton R. A common structural motif incorporating a cystine knot and a triple-stranded beta-sheet in toxic and inhibitory polypeptides. Protein Sci 1994;3:1833–6.
[21] Pimentel C, Choi SJ, Chagot B, Guette C, Camadro JM, Darbon H. Solution structure of PcFK1, a spider peptide active against *Plasmodium falciparum*. Protein Sci 2006;15:628–34.
[22] Reily MD, Holub KE, Gray WR, Norris TM, Adams ME. Structure–activity relationships for P-type calcium channel-selective w-agatoxins. Nat Struct Biol 1994;1:853–6.
[23] Stewart JM, Young JD. Solid phase peptide synthesis; 1969.
[24] Stigter D, Dill KA. Charge effects on folded and unfolded proteins. Biochemistry 1990;29:1262–71.
[25] Thongyoo P, Roque-Rosell N, Leatherbarrow RJ, Tate EW. Chemical and biomimetic total syntheses of natural and engineered MCoTI cyclotides. Org Biomol Chem 2008;6:1462–70.
[26] Thongyoo P, Tate EW, Leatherbarrow RJ. Total synthesis of the macrocyclic cysteine knot microprotein MCoTI-II. Chem Commun (Camb) 2006;2848–50.
[27] Wang X-H, Connor M, Wilson D, Wilson HI, Nicholson GM, Smith R, et al. Discovery and structure of a potent and highly specific blocker of insect calcium channels. J Biol Chem 2001;276:40306–12.